ARCHIVES of FOUNDRY ENGINEERING
DOI: 10.2478/afe-2014-0022
Published quarterly as the organ of the Foundry Commission of the Polish Academy of Sciences
ISSN (2299-2944)
Volume 14
Issue 1/2014
97 – 102

Analysis of the Crystallization of AZ91 Alloy by Thermal and Derivative Analysis Method Intensively Cooled in Ceramic Shell

C. Rapiejko [a,] *, B. Pisarek [a], E. Czekaj [b], T. Pacyniak [a]
[a] Lodz University of Technology, Department of Materials Engineering and Production Systems, ul. Stefanowskiego 1, 90-924 Łódź, Poland
[b] Foundry Research Institute, ul. Zakopiańska 73, 34-120 Kraków, Poland
* Corresponding author. E-mail address: cezary.rapiejko@p.lodz.pl

Received 30.06.2013; accepted in revised form 02.09.2013

Abstract

The work presents the test result of the influence of cooling rate on the microstructure of AZ91 alloy, Vickers micro-hardness and Brinell hardness. Studies cooling and crystallization of AZ91 alloy was cast into the ceramic shells pre-heated to 180 ° C and then air-cooled at ambient temperature or intensively super cooled in the liquid coolant. The TDA method was applied to record and characterize the thermal effect resulting from the phase transformations occurring during the crystallization of AZ91 alloy. The kinetics and dynamics of the thermal processes of crystallization of AZ91 alloy in the ceramic shells were determined. Metallographic tests were performed with the use of an optical microscope. A comparison of these test results with the thermal effect recorded by way of the TDA method was made. Influence of cooling rate of AZ91 on $HV_{0,01}$ micro-hardness and Brinell hardness alloy was examined.

Keywords: Innovative casting materials and technologies, Magnesium alloys, TDA method, Micro hardness, Hardness, Sophia®, Hero Premium CASTING®

1. Introduction

Technology of the investment casting method using ceramic shells has been known for many years. It is characterized by volumetric crystallization which have detrimental effects the mechanical properties of castings. In the recent years, new casting technologies characterized by directional crystallization and providing heat dissipation rapidly from the ceramic shells have been developed. The most common ones used to obtain castings of titanium and aluminum are two technologies SOPHIA ® [1] and the second HERO Premium Casting ® [2,3]. The SOPHIA ® technology has been also applied to production of magnesium alloy castings [4]. In the world literature, there are no reports on the research of crystallization of alloys super cooled in the liquid coolant by the TDA method. The TDA method is commonly used for testing air-cooled alloys. This method allows for the determination of the kinetics and dynamics of the thermal processes of metal solidification. It is applied for the analysis of the alloys of both the ferrous [5] and the non-ferrous metals [6,7] included bronzes [8-10]. The TDA tests of Mg alloys are conducted in metal crucibles [11-13]. Magnesium alloy castings are obtained by investment casting method in ceramics shells [9], which characterize in a much lower heat conductivity coefficient, and so the solidification and the crystallization process is different than that in the metal moulds. The use intensive liquid cooling of casting significantly speed up the process of crystallization. In the world literature are no reports of studies of solidification and

crystallization of AZ91 alloy in a ceramic shell air-cooled or liquid-cooled used in the investment casting method.

The aim of this work was to test of investigate the effect of cooling rate of AZ91 alloy cast in a ceramic shells in the air-cooled or intensively liquid cooled in a 30% solution of Polihartenol E8 in water on the microstructure, micro-hardness $HV_{0,01}$ and Brinell hardness. The tests of solidification and crystallization of AZ91 alloy in the ceramic ATD10C-PŁ probe air cooled or super intensively liquid cooled has been conducted on measuring station developed at the Department of Materials Engineering and Production Systems of Lodz University of Technology by the TDA method.

2. Test methodology

The chemical composition of the AZ91 alloy is shown in Table 1.

Table 1.
Chemical composition of alloy AZ91

Skład chemiczny, % mas							
Mg	**Al**	**Zn**	**Mn**	**Si**	**Fe**	**Cu**	**Ni**
90.027	9	0.8	0.1	0.05	0.004	0.008	0.001

The TDA method was applied to test the solidification and crystallization process of AZ91, produced in specially designed ceramic probes. The ceramic shells of the probes were made according to the technology of ceramic shell production in the investment casting method applied in the obtaining of aluminium alloy casts [15].

The ceramic shells of the TDA probes were made of refractory REFRACORSE flour and sands. The shells consisted of 7 coatings made in mixers and in a fluidizer, at the „Armatura" Foundry in Łódź, Poland. Each coating was created as a result of applying a binder on the wax model and next covering it with quartz sand of a particular granularity. Figure 1 presents the ceramic ATD10C-PŁ probe used during the tests.

Fig. 1. Ceramic ATD10C-PŁ probe

After the desiccation, a model mass was melted from the ceramic shell in an autoclave at 150 °C. Next, the shell was reinforced at 960 °C in a tunnel furnace. After the burning, the ceramic samples were cooled down to 180 °C, and then liquid 800 °C ± 5 °C metal was cast on them.

The metal was melted in a laboratorial crucible resistance furnace of 5 kg capacity. The crucible was made of S235JRG2 steel – standard PN-EN 10025-2:2005. Inside the furnace, protective gas atmosphere was used which consisted of an Ar + SF_6 mixture with the pressure of 0.15 -0.20 MPa. The gas flow equaled 10 cm^3/min for SF_6 and 500 cm^3/min for Ar.

The configuration and the type of the used coatings is presented in Table 2.

Table 2.
Coating characteristics

Coating no.	Viscosity [s]	Binder type	Sand granularity [mm]
1	38	Ludox	0.1 – 0.3
2	20	Ludox	0.1 – 0.3
3	17	Ethyl silicate	0.2 – 0.5
4	18	Ethyl silicate	0.5 – 1.0
5	19	Ludox	0.5 – 1.0
6	18	Ethyl silicate	0.5 – 1.0
7	20	Ethyl silicate	0.5 – 1.0

As a coolant used 30% solution of Polihartenol E8 in H_2O at ambient temperature t_{ot} = 20 °C.

The recording of the TDA characteristics was performed at a working station, whose scheme can be seen in Figure 2.

One of the elements of the working station is a TDA stand, in which a measuring thermoelement type K was installed (NiCr-NiAl). The thermoelement was connected with an analogue-digital converter, Crystaldigraph, which converted the voltage signal into a frequency one, which was then recorded by the computer.

The evaluation of the cooling ($t=f(\tau)$), kinetics ($dt/d\tau=f'(\tau)$) and dynamics ($d^2t/d\tau^2= f''(\tau)$) of the crystallization processes was performed by the TDA method. On the derivative curve $dt/d\tau= f'(\tau)$ the following thermal effects were marked AZ91 alloy:

Pk-A-D - crystallization of primary α_{Mg} phase ($L \rightarrow L+\alpha_{Mg}$),

D-E-F-H - crystallization of $\alpha_{Mg}+\gamma(Mg_{17}Al_{12})$ eutectic ($L \rightarrow \alpha_{Mg}+ \gamma(Mg_{17}Al_{12})$).

In the description of the characteristics of the thermal processes occurring during the primary crystallization, the following quantities were applied:

the temperature of the alloy (liquid metal), with the recording of the characteristic points t, °C,

- the value of the first derivative of the temperature after the time for these points $dt/d\tau$, °C/s,
- the value of the tangent of the inclination angle of the straight line at the interpolated interval between the characteristic points $tg(\alpha) \approx d^2t/d\tau^2$, °C/$s^2$,
- the time which passed from the beginning of the measurement of the occurrence of the characteristic points on the derivative curve (crystallization curve) τ, s.

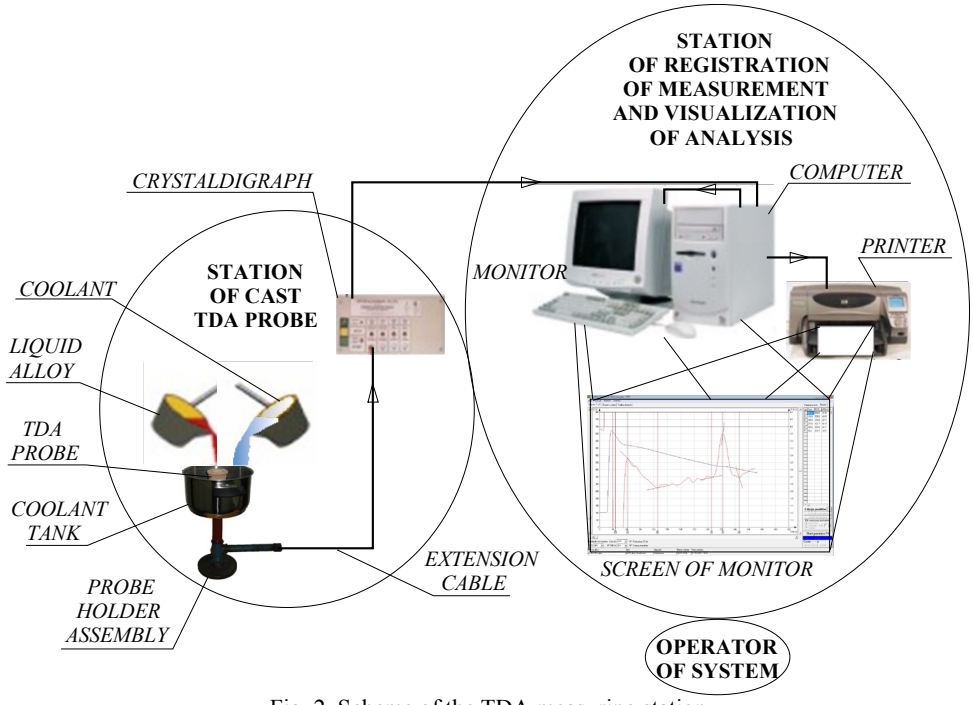

Fig. 2. Scheme of the TDA measuring station

In order to demonstrate the particular phases in the microstructure, the microsections were etched with a reagent of the following composition: 1 ml acetic acid, 50 ml distilled water and 150 ml ethyl alcohol [13]. The microstructure of the samples of AZ91 alloy was observed by means of the Nikon Eclipse MA200 optical microscope.

The Vickers micro hardness tests were performed on micro hardness tester VH-1000 using a scale of hardness HV 0.01. The Brinell hardness tests were performed on the Brinell hardness tester with load of 490N and the diameter of the ball penetrator diameter = 2.5 mm.

3. Result description

3.1. Results of AZ91 alloy

In Figures 3 and 4 show the characteristics TDA AZ91 alloy solidification in the ceramic ATD10C-PŁ probe respectively:

- of cooling in ambient air (Fig. 3),
- intensively cooled in a 30% solution of Polihartenol E8 in H_2O from temperature of 570 °C (Fig. 4).

On the derivative curve (dt/dτ) points: Pk, A, D and E designate the thermal effect of crystallization phase α_{Mg} (in volume of probe), E, F and H determine the effect of heat eutectic crystallization $\alpha_{Mg} + \gamma(Mg_{17}Al_{12})$.

After the metal supercooling, below the equilibrium liquidus temperature, nucleate and grow grains of phase α_{Mg} in the actual liquidus temperature tA=569 °C (Fig. 3). The intensity of the cooling rate changes in the initial stage of crystallization of grains phase α_{Mg} is ZPK=184.06·10^{-3} °C/s^2. After reaching in point A of maximum thermal effects of crystallization phase α_{Mg} intensity of changes of the cooling rate is reduced to ZA = -6.71·10^{-3} °C/s^2. Not all of the volume of the liquid alloy crystallizes as phase α_{Mg}. The duration of the thermal effect of Pk-A-D is $SK_{PK-D}=\tau D-\tau Pk$ =92.8 s. Thermal effect Pk-A-D comprises the step of intense nucleation and growth of phase α_{Mg}, the kinetic of thermal processes (dt/dτ) of growth of phase α_{Mg}, on the section between points D and E, strongly decreases. The dynamics of thermal processes for the point D is comparable with the dynamics of these processes to the point E, ZD=ZE=1,30·10^{-3} °C/s^2. At this stage, ahead the crystallization front of phase αMg, in a liquid alloy slowly increasing the concentration of Al, which in turn leads to nucleation and growth of eutectic $\alpha_{Mg}+\gamma(Mg_{17}Al_{12})$. After the undercooling of alloy, below the equilibrium temperature of eutectic transformation in the actual transformation temperature tF=422 °C nucleates and grows eutectic $\alpha_{Mg}+\gamma(Mg_{17}Al_{12})$. The dynamics of thermal processes eutectic crystallization is, respectively: before the maximum thermal effects of crystallization ZF= 53.58·10^{-3} °C/s^2, after the maximum ZH=-40.01·10^{-3} °C/s^2. AZ91 alloy solidified in the volume of ATD10C-PŁ probe by the time $SK_{Pk-H}=\tau_H-\tau_{Pk}$=274,4 s, of which the phase α_{Mg} crystallization lasted $SK_{Pk-E}=\tau_E-\tau_{Pk}$=210,4 s and eutectic crystallization $\alpha_{Mg}+\gamma(Mg_{17}Al_{12})$ $SK_{E-H}=\tau_H-\tau_E$=64,0 s.

Intensive cooling of the alloy AZ91 in the ATD10C-PŁ probe obtained after reaching the alloy temperature t=570 °C, it is real liquidus temperature tA, defined in the previous measurement (Fig. 3), by filling the coolant tank. As might be expected, the characteristic temperature of the phase transformation moves towards lower values, increases the crystallization dynamics of thermal processes and the duration of phase transformations is reduced. After supercooling AZ91 alloy intensively cooled below

the equilibrium liquidus temperature, nucleate and grow grains of α_{Mg} phase in a real liquidus temperature of tA=555 °C (Fig. 4).

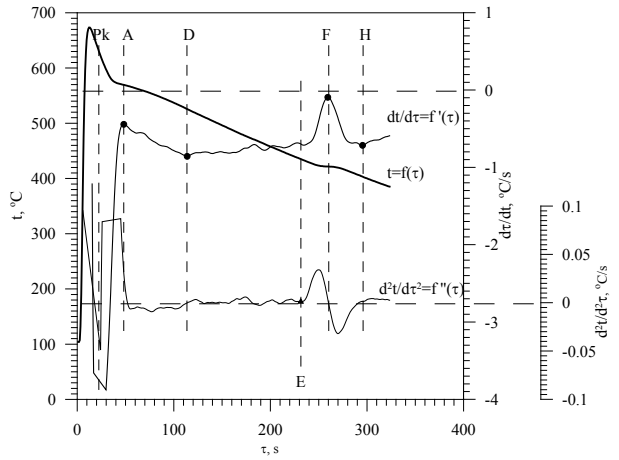

Point	Pk	A	D	E	F	H
τ, s	21.0	48.2	113.8	231.4	259.4	295.4
t, °C	638	569	526	435	422	403
dt/dτ, °C/s	-4.94	-0.44	-0.86	-0.70	-0.09	-0.72
$Z\approx d^2t/d\tau^2$, $*10^{-3}$ °C/s²	184.06	-6.71	1.30	1.30	53.58	-40.01

Fig. 3. Characteristics of TDA of AZ91 alloy solidifying in ceramic ATD10C-PŁ probe

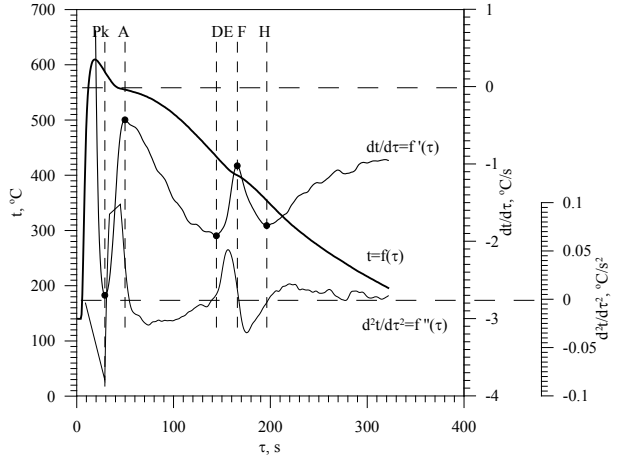

Point	Pk	A	D=E	F	H
τ, s	29.0	49.8	144.2	165.8	196.2
t, °C	588	555	434	400	354
dt/dτ, °C/s	-2.70	-0.43	-1.93	-1.02	-1.80
$Z\approx d^2t/d\tau^2$, $*10^{-3}$ °C/s²	189.22	-25.51	-	76.54	-41.10

Fig. 4. Characteristics of TDA of AZ91 alloy solidifying in ceramic ATD10C-PŁ probe, cooled from a temperature of 570 °C in a 30% solution of Polihartenol E8 in H_2O

The intensity of the cooling rate changes in the initial stage of crystallization of grains of α_{Mg} phase is ZPK=189.22·10^{-3} °C/s^2. After reaching in point A of maximum thermal effects of crystallization of α_{Mg} phase intensity changes the cooling rate is reduced to ZA=-25.51·10^{-3} °C/s^2. Not all of the volume of the liquid alloy crystallizes as α_{Mg} phase. The duration of the thermal effect of Pk-A-D is $SK_{Pk-D}=\tau_D-\tau_{Pk}$=115,2 s. Pk-A-D-thermal effect comprises the step of intense nucleation and growth of α_{Mg} phase. Rapid cooling of the ATD10C-PŁ probe led to elimination of the section between points D and E (D = E), where the slower pace of cooling the alloy in the ceramic shell kinetics of thermal processes (dt/dτ) growth of α_{Mg} phase strongly decreases.

Therefore, ahead the crystallization front of α_{Mg} phase, in a liquid alloy rapidly increasing the concentration of Al, which in turn leads to nucleation and growth of eutectic $\alpha_{Mg}+\gamma(Mg_{17}Al_{12})$. Eutectic $\alpha_{Mg}+\gamma(Mg_{17}Al_{12})$ nucleates and grows in the alloy after supercooling liquid below the eutectic equilibrium transformation temperature, the actual transition temperature tF=400 °C. The dynamics of thermal processes eutectic crystallization is, respectively: before the maximum of thermal effects of crystallization ZF=76.54·10^{-3} °C/s^2, after the maximum ZH=-41.10·10^{-3} °C/s^2. AZ91 alloy solidified in the volume ATD10C-PŁ probe durable $SK_{Pk-H}=\tau H-\tau Pk$=167.2 s, of which the crystallization α_{Mg} phase durable $SK_{Pk-E}=\tau E-\tau Pk$=115.2 s and eutectic crystallization $\alpha_{Mg}+\gamma(Mg_{17}Al_{12})$ $SK_{E-H}=\tau H-\tau E$=52.0 s.

In Figures 5 and 6 shows the microstructure of AZ91 alloy solidifying in the ATD10C-PŁ probe respectively:

- of cooling in ambient air (Fig. 5 a,b),
- intensively cooled in a 30% solution of Polihartenol E8 in H_2O from temperature of 570 °C (Fig. 6 a,b).

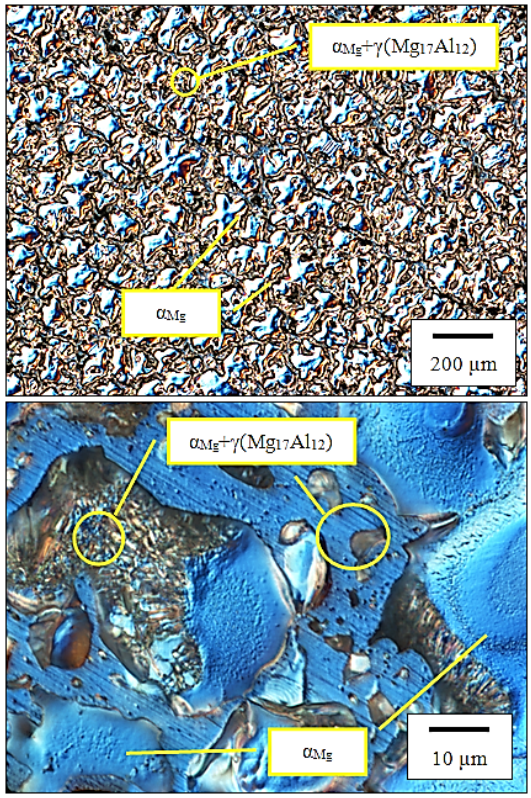

Fig. 5. Microstructure of AZ91 alloy solidifying in the ATDC-10PŁ probe (cooling of ambient air)

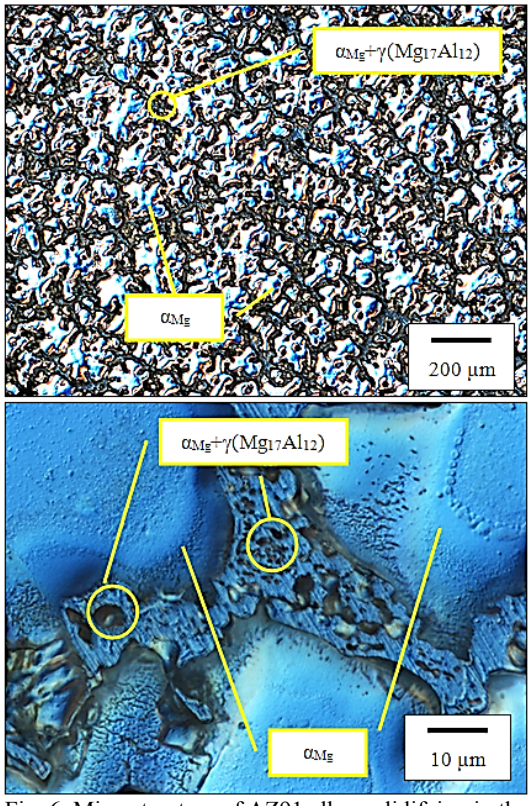

Fig. 6. Microstructure of AZ91 alloy solidifying in the ATDC-10PŁ probe (intensive cooling in a 30% solution of Polihartenol E8 in H_2O from temperature 570 °C)

Microstructure of AZ91 alloy, solidifying in the ATD10C-PŁ probe, of cooling by ambient air is composed of phases: α_{Mg} + eutectic (α_{Mg}+$\gamma(Mg_{17}Al_{12})$). Its main characteristic is the presence of eutectic in microstructure α_{Mg}+$\gamma(Mg_{17}Al_{12})$, both in the form of lamellar and massive γ phase precipitates ($Mg_{17}Al_{12}$) with internal, approximated the shape of the sphere α_{Mg} phase precipitates (Fig. 5b).

Microstructure of AZ91 alloy solidifying in the ATD10C-PŁ probe intensively cooled in a 30% solution of Polihartenol E8 in H_2O from temperature of 570 °C, is also composed of phases: α_{Mg} +eutectic (α_{Mg}+$\gamma(Mg_{17}Al_{12})$) (Fig. 6 a, b). However, this alloy is no longer present eutectic α_{Mg}+$\gamma(Mg_{17}Al_{12})$ in the form of lamellar, a characteristic of the alloy microstructure formed during slow cooling (in ambient air) in the ceramic shell (Fig. 5b). However, separation of solid phase γ ($Mg_{17}Al_{12}$) are narrower, with the inner more fragmented α_{Mg} phase precipitates (Fig. 6b).

Hardness HB of test alloy solidifying in the ATD10C-PŁ ceramic shell, shown in Figure 7 and the microhardness $HV_{0.01}$ phases or their systems, characteristic for the microstructure in Figure 8.

Registered increase in hardness of the test alloy solidifying in the probe ceramic, which is cooled in ambient air, with about 63HB to about 68HB after the intensive cooling in a 30% solution of Polihartenol E8 in H_2O from temperature of 570 °C (Fig. 7). This represents an increase of about 8%. The reason for this is primarily a higher supercooling of alloy during crystallization.

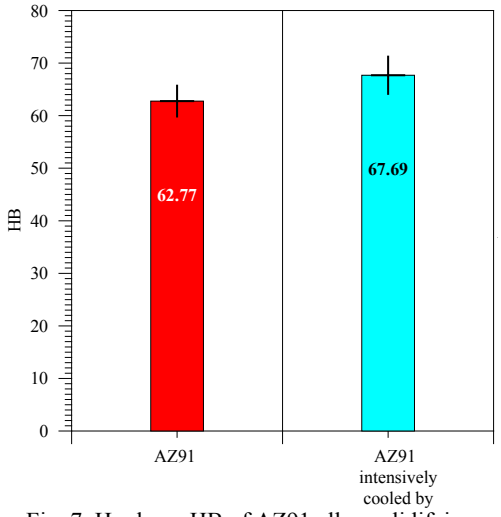

Fig. 7. Hardness HB of AZ91 alloy solidifying in the ATDC-10PŁ probe

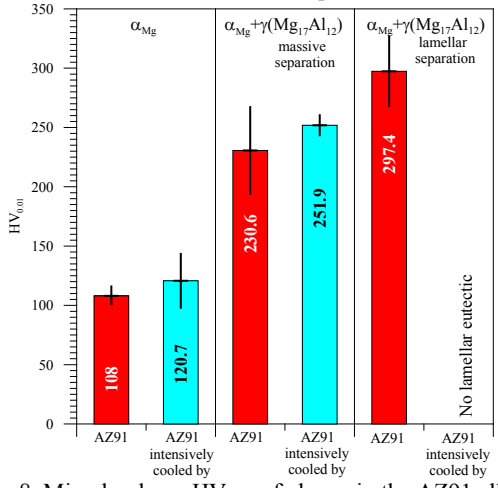

Fig. 8. Microhardness $HV_{0.01}$ of phases in the AZ91 alloy solidified in the ATDC-10PŁ probe

As a result, there was increase of supercooling occurred to increase supersaturation α_{Mg} phase of additions of: Al, Zn or Mn, and fragmentation of solid precipitates of γ phase ($Mg_{17}Al_{12}$) (Fig. 6 a,b) as compared to the alloy cooled in ambient air (Fig. 5 a,b). The increase in saturation phase α_{Mg} of additives, as well as fragmentation of γ phase ($Mg_{17}Al_{12}$) resulted in an increase of microhardness (Fig. 8).

4. Conclusions

From the tests presented in this work, we can conclude that:

- used to study ceramic ATD10C-PŁ probes allow for examination of solidification and crystallization of castings:
  - in conditions similar to those occurring in the real ceramic shells used in implementing the method of lost wax casting models,

    - under conditions of intense cooling of the real ceramic shells,
- intensive cooling of AZ91 alloy in 30% solution of Polihartenol E8 in H_2O from temperature of 570 °C allows you to:
    - increase the hardness of HB by about 8% relative to alloy of cooling in ambient air,
    - increase the microhardness HV phases: α_{Mg} and eutectic $\alpha_{Mg} + \gamma$ ($Mg_{17}Al_{12}$),
- it is possible to apply and implement methods of the ATD to control the properties magnesium alloy castings intensively cooled in the ceramic shell.

Acknowledgements

This work was realized within the frames of Project PBS I, financed by the National Centre for Research and Development, Project ID: 178739. Project implemented in 2013-2015.

References

[1] Gabriel, J. (1996). Entwicklungen bei Aluminium-Feinguss - Moeglichkeiten des SOPHIA® - Verfahrens. *Konstruieren + Giessen.* 1, 4-10.
[2] Liesner, Ch. & Gerke-Cantow, R. (2002). Aluminium-Feinguss nach dem HERO Premium Casting – Verfahren. *Konstruieren + Giessen.* 27(2), 41-44.
[3] Liesner, Ch. & Gerke-Cantow, R. (2002). Aluminium-Feinguβ nach dem HERO Premium Casting ® - Verfahren. *Konstrusieren + Giβen.* 27(2), 41-44.
[4] http://www.aeromet.co.uk/casting-division/index.html
[5] Gumienny, G. (2011). TDA method application to austenite transformation in nodular cast iron with carbides assessment. *Archives of Foundry Engineering.* 11(3), 159-166.
[6] Kacprzyk, B., Szymczak, T., Gumienny, G. & Klimek, L. (2013). Effect of the Remelting on Transformations in Co-Cr-Mo prosthetics Alloy. *Archives of Foundry Engineering.* 13(3), 47-50.
[7] Pietrowski, S. & Szymczak, T. (2010). Crystallization, microstructure and mechanical properties of silumins with micro-additions of Cr, Mo, W and V. *Archives of Foundry Engineering.* 10(1), 123-136.
[8] Pietrowski, S. & Pisarek, B. (2007). Computer-aided technology of melting high-quality metal alloys. *Archives of Metallurgy and Materials*. 52(3), 481-486.
[9] Pisarek, B. (2010). Influence of the technology of melting and inculation preliminary alloy AlBe5 on change of concentration of Al and micro-structure of the bronze CuAl10Ni5Fe4. *Archives of Foundry Engineering*. 10(2), 127-134.
[10] Pisarek, B. (2013). Model of Cu-Al-Fe-Ni Bronze Crystallization. *Archives of Foundry Engineering*. 13(3), 72-79.
[11] Dobrzański, L. A., Tański, T., Dobrzańska-Danikiewicz, A. D., Król, M., Malara, Sz. & Domagała-Dubiel, J. (2012). *Structure and properties of Mg-Al-Zn alloys*. Chapter 3. Derivative and thermal analysis of Mg-Al-Zn alloys. Open Access Library. 5(11), 44-77.
[12] Braszczyńska-Malik, K. N. & Zyska, A. (2010). Influence of solidification rate on microstructure of gravity cast AZ91 magnesium alloy. *Archives of Foundry Engineering*. 10(1), 23-26.
[13] Lun Sin, S., Dubé, D. & Tremblay, R. (2008). An investigation on microstructural and mechanical properties of solid mould investment casting of AZ91D magnesium alloy. *Materials Characterization*. 59, 178-187.
[14] Zhiyong, Y., Yuhua, Z., Weili, Ch., Jinshan, Z. & Yinghui, W. (2012). Effect of Cu addition on microstructure and properties of Mg-10Zn-5Al-0.1Sb high zinc magnesium alloy. *China Foundry, Research & Development*. February, 43-47.
[15] Pietrowski, S. & Rapiejko, C. (2011). Temperature and microstructure characteristics of silumin casting AlSi9 made with investment casting method. *Archives of Foundry Engineering*. 11(3), 177-186.
[16] Maltais, D., Dube, M., Fiset, G., Laroche, S. & Turgeon, (2004). Improvements in the metallography of as-cast AZ91 alloy. *Material Characterization.* 52, 103-119.